BEAM
INTERACTIONS
WITH
MATERIALS
AND ATOMS

Measurement of the ^{7}Li(p,p'γ)^{7}Li reaction cross-section and 478 keV photon yield from a thick lithium target at proton energies from 0.65 MeV to 2.225 MeV

Sergey Taskaev [b,*], Timofey Bykov [a,b], Dmitrii Kasatov [a,b], Iaroslav Kolesnikov [a,b], Alexey Koshkarev [a,b], Alexandr Makarov [a,b], Sergey Savinov [a,b], Ivan Shchudlo [a,b], Evgeniia Sokolova [a,b]

[a] *Budker Institute of Nuclear Physics, 11 Lavrentiev ave, 630090 Novosibirsk, Russia*
[b] *Novosibirsk State University, 2 Pirogov str, 630090 Novosibirsk, Russia*

A R T I C L E   I N F O

A B S T R A C T

Reliable data on ^{7}Li(p,p'γ)^{7}Li reaction cross section and photon yield from a thick lithium target are important for many applications including boron neutron capture therapy of malignant tumors. Experimental data on cross section differ greatly from one author to another; experimental data on photon yield are extremely scarce. Measurements of the reaction cross section and photon yield were carried out at the accelerator-based neutron source at the Budker Institute of Nuclear Physics (Novosibirsk, Russia) using a NaI and HPGe γ-ray spectrometers. The ^{7}Li(p,p'γ)^{7}Li reaction cross section and 478 keV photon yield from a thick lithium target at proton energies from 0.65 MeV to 2.225 MeV have been measured with high accuracy. The data obtained are presented in the form of tables.

1. Introduction

The concept of Boron Neutron Capture Therapy (BNCT) [1] is to provoke inside cancerous cells a nuclear reaction between accumulated boron-10 nuclei and thermal neutrons for which the absorption cross section is extremely high. Thus, the cancerous cells can be destroyed by the resulting nuclei with high linear energy transfer [2]. Two different neutron beams are commonly used for BNCT: the thermal neutron beam which limits the treatment to shallow tumors, such as skin melanoma, and the harder epithermal neutron beam for deep-seated tumors such as glioblastoma multiform. The last one can penetrate deeper into tissues due to its high energy and can reach the thermal energy range after being slowed down by tissues. Epithermal beams thus allow patient treatment without surgical resection.

It is generally recognized that the generation of neutrons as a result of the ^{7}Li(p,n)^{7}Be threshold reaction at proton energies in the region of 2.3–2.5 MeV allows forming a neutron beam that best meets the requirements of BNCT [1–3]. The use of a lithium target entails additional emission of 478 keV photons as a result of inelastic scattering of a proton by lithium nuclei (^{7}Li(p,p'γ)^{7}Li reaction). Accompanying photon absorbed dose is undesirable for BNCT. Knowing the photon yield of the ^{7}Li(p,p'γ)^{7}Li reaction is certainly important for nuclear data evaluation and for estimating the absorbed dose when planning therapy. However, the data of the 478 keV photon yield and the data of the ^{7}Li(p,p'γ)^{7}Li reaction cross section in the literature [4–16] differ significantly. Fig. 1 shows the data of 478 keV photon yield in the ^{7}Li(p,p'γ)^{7}Li reaction, and Fig. 2 shows the data of the ^{7}Li(p,p'γ)^{7}Li reaction crosssection.

The aim of this work is to measure cross-section of the ^{7}Li(p,p'γ)^{7}Li reaction and 478 keV photon yield from a thick lithium target.

2. Experimental facility

The study was carried out on an accelerator-based neutron source at the Budker Insitute of Nuclear Physics in Novosibirsk, Russia [17]. The layout of the experimental facility is shown in Fig. 3. The DC tandem accelerator *1* is used to provide a proton beam of 1 cm diameter directed to a lithium target *4*. Lithium target has three layers: a layer of pure lithium to generate neutrons in ^{7}Li(*p,n*)^{7}Be reactions; a layer of material resistant to radiation blistering; and a copper substrate for efficient heat removal [18]. Vacuum evaporation of lithium on the target is carried out
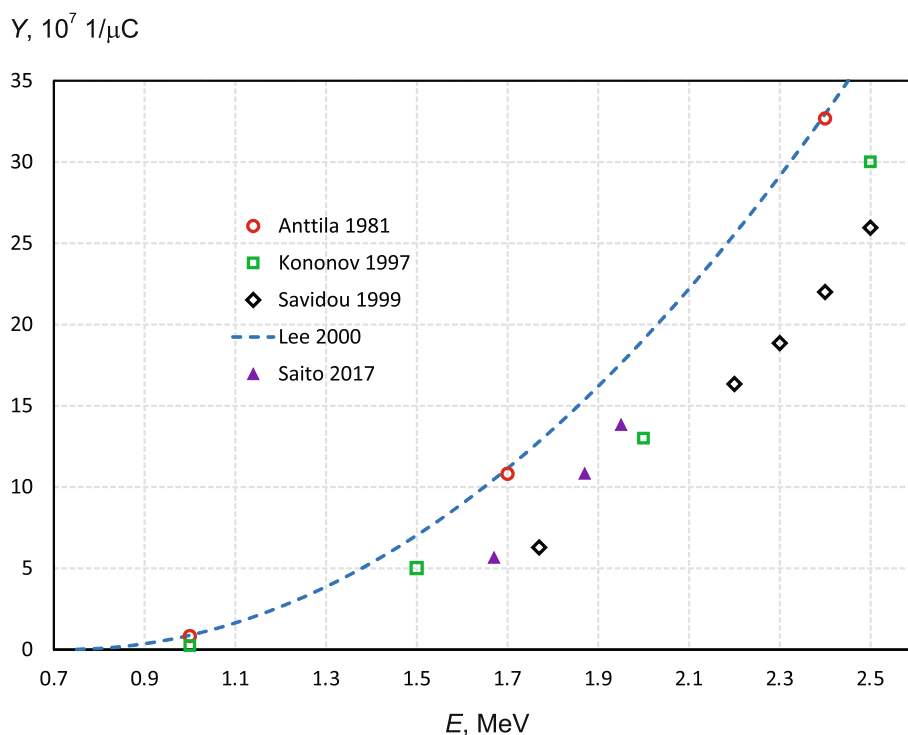
Fig. 1. Yield of 478 keV photon in the ^{7}Li(p,p'γ)^{7}Li reaction: ○ – measured [4], □ – calculated [5], ◇ – measured at $E = 1.75$ MeV and calculated at other energy values [6], - - - – calculated [7], Δ – measured at $E = 1.67$ MeV and 1.87 MeV and estimated at 1.95 MeV [8].
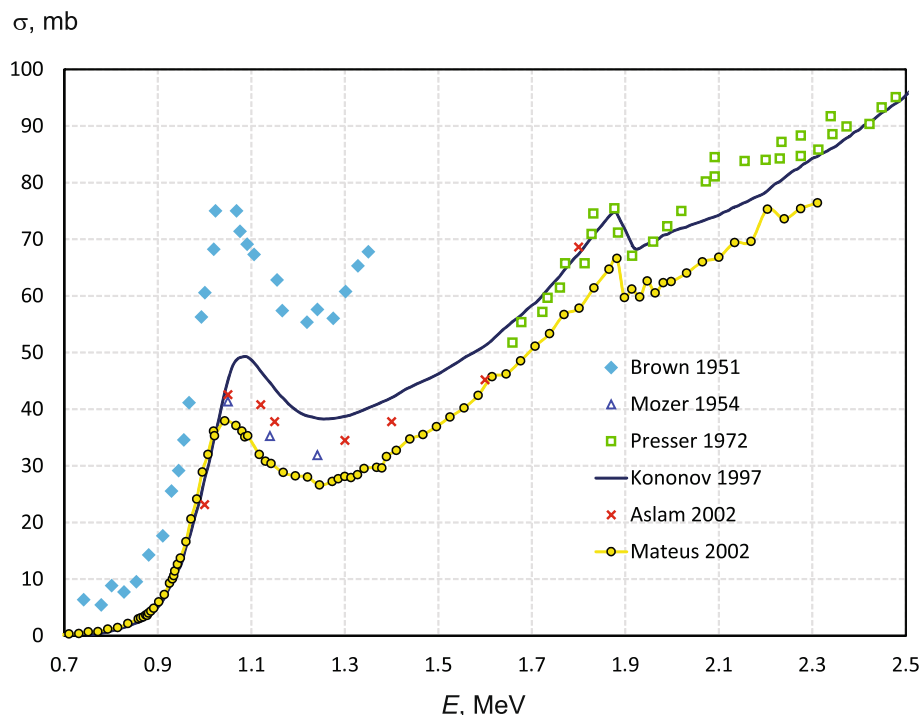

Fig. 2. ^{7}Li(p,p'γ)^{7}Li reaction cross-section [5,9–14].

at a separate stand. After lithium deposition, the target unit together with a part of vacuum chamber *3*, closed with a gate valve to maintain vacuum inside, is disconnected from the lithium evaporation stand, transferred to the experimental facility and connected to the horizontal proton beam line.

Proton current is measured and controlled by a non-insertion DC current transformer NPCT (Bergoz Instrumentation, France) *2*. The

position and size of the proton beam on the surface of the lithium target are measured and controlled by the Hikvision video camera installed on the window *5* and eight thermocouples inserted into the holes inside the target drilled from the side surface.

When lithium was evaporated, we used natural lithium produced by the Novosibirsk Chemical Concentrates Plant; in the batch used, the percentage of lithium was 99.956%. The percentage of lithium-7 in
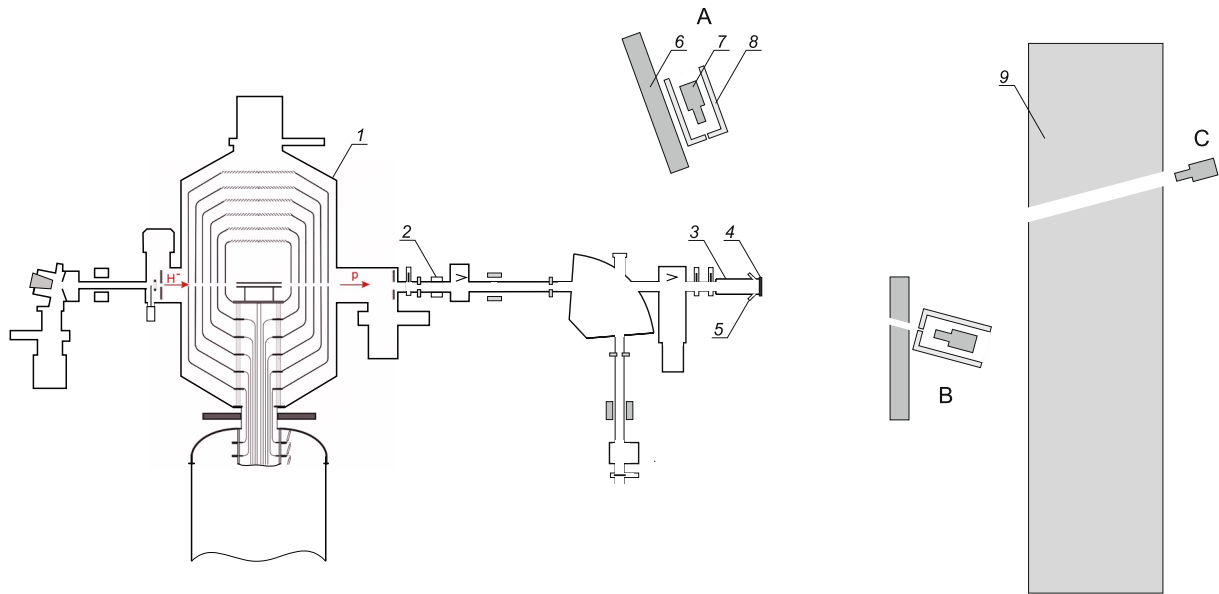
Fig. 3. Layout of the experimental facility (the drawing is not to scale): *1* – vacuum insulated tandem accelerator, *2* – non-insertion DC current transformer, *3* – target unit, *4* – lithium target, *5* – view port, *6* – temporary concrete wall, *7* – gamma-ray spectrometer, *8* – lead collimator, *9* – concrete wall.
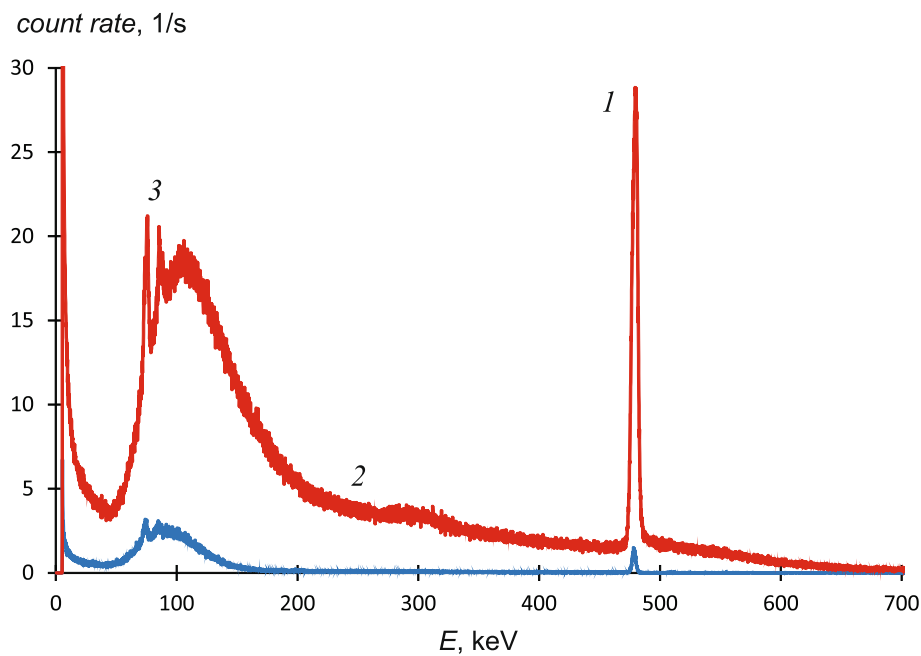
Fig. 4. Typical signal of HPGe gamma-ray spectrometer: *1* – 478 keV photons emitted in ^{7}Li(p,p'γ)^{7}Li reaction, *2* – bremsstrahlung of the accelerator, *3* – characteristic X-rays emitted by lead. The upper curve was obtained at a proton energy of 1.75 MeV, the lower one at 0.8 MeV.

natural lithium varies from 92.41% [19] to 92.58% [20]; we will assume the lithium-7 content is equal to the average value, namely 92.5%.

The intensity of γ-radiation is measured, according to the experimental needs, by a high purity germanium γ-ray spectrometer (SEG-1KP-IPTP 12 from Institute of Physical and Technical Problems, Dubna, Russia) and/or a 51 mm $\times$ 51 mm NaI(Tl) scintillator (Azimut Photonics, Russia; supplier of scintillator – the Saint-Gobain Crystals).

The measurements were carried out with 3 options for placing the γ-spectrometer; in Fig. 3 they are shown as A, B, and C. In positions A and B the spectrometer is placed inside the lead collimator *8* with external diameter of 270 mm, 500 mm length and 50 mm wall thickness. Together with the collimator, the spectrometer is protected from a bremsstrahlung of the accelerator by a 23 cm thick wall *6* built of

concrete blocks. In position C, the spectrometer is placed in an adjacent bunker behind a 1.47 m thick concrete wall. A hole was specially made in the wall aimed at the target. Note that the location of the concrete wall, collimator and spectrometer is shown in Fig. 3 schematically; in reality they are located in the horizontal plane.

In the next chapter, the results of measurements taken in A, B, and C positions will be presented sequentially. This sequence of presentation of the results is chronological, motivated by the need of checking the isotropy of the radiation (done in B position), and improving the accuracy of measurements (done in C position).
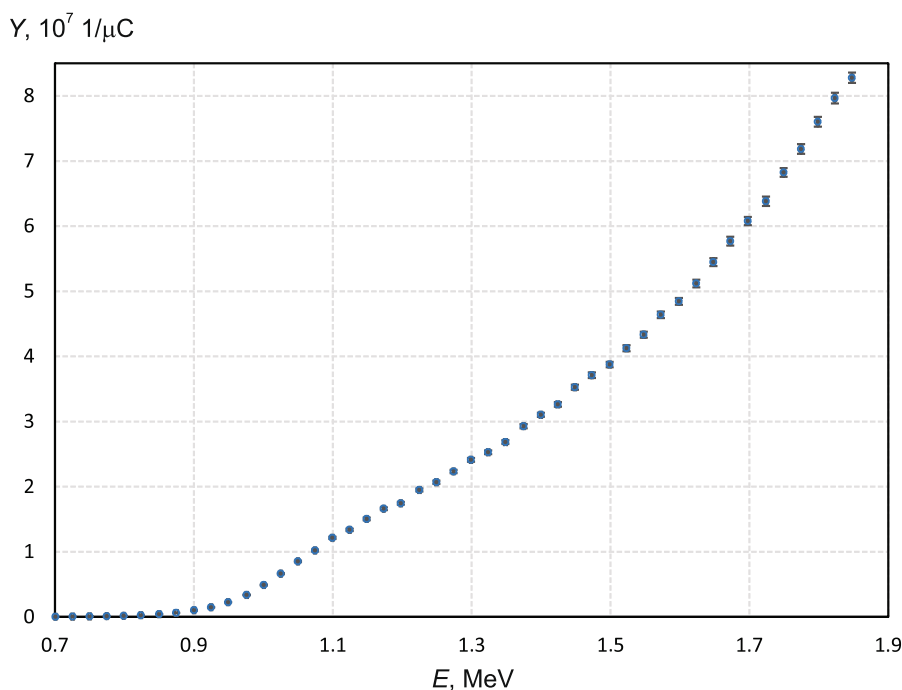
Fig. 5. Measured yield of 478 keV photons from a thick natural lithium target.
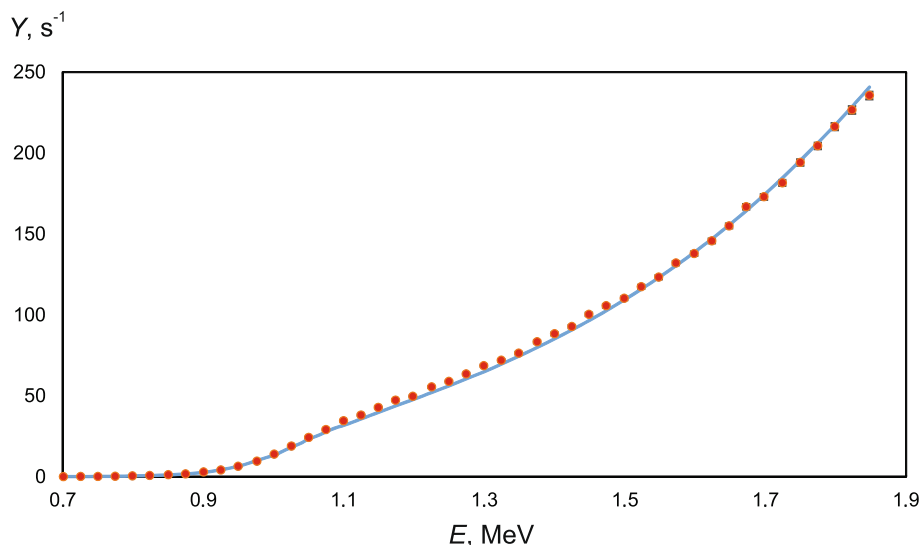

Fig. 6. Dependence of the 478 keV photon count rate on proton energy E: circles – measured from a thick lithium target, line – recovered from measurements from a thin 2.1 µm lithium target.

3. Results and discussion

3.1. Position A

First, measurements were taken at position A. The sensitive part of the spectrometer is located at a distance of 2.00 m at an angle of 110°. A typical signal of the HPGe gamma-ray spectrometer is shown in Fig. 4. It shows a narrow useful signal in the region of 478 keV, a broad signal due to bremsstrahlung of the accelerator, the intensity of which increases with increasing accelerator voltage, and characteristic X-rays emitted by lead in the region below 90 keV. The dead time of the spectrometer did not exceed 26% when measuring the reaction cross section and 13.4% when measuring the photon yield.

HPGe γ -ray spectrometer is calibrated on total sensitivity by closed type Cs-137 radionuclide source of photon radiation with activity $1.6 \cdot 10^8$ Bq (10% accuracy) in 661.657 keV line. During calibration the radionuclide source was placed on the surface of the copper disk in its center – as close as possible to the lithium layer. The relative sensitivity of the HPGe γ-ray spectrometer was calibrated by the following reference sources of photon radiation from the OSGI-TR set (Ritverc, Russia): Na-22, Mn-54, Co-60, Ba-133, Cs-137, Eu-152 and Bi-207. Intensity reliability of reference radiation sources is 7%. Finally, the absolute efficiency at 478 keV was fixed by interpolating the data obtained.

The experimental result of the 478 keV photon yield from a thick lithium target at proton energies from 0.7 to 1.85 MeV with 25 keV step is presented in Fig. 5. The target is called thick if the thickness of the evaporated lithium layer exceeds the proton range in lithium. The proton range is equal to 31 µm at proton energy 0.7 MeV and 144 µm at
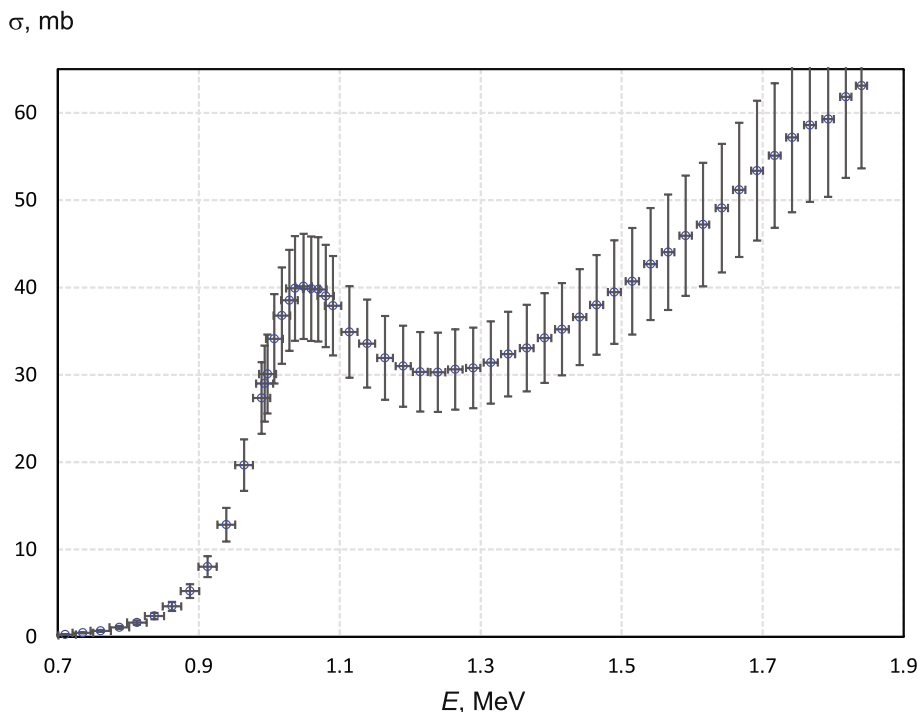
σ, mb

Fig. 7. Cross section of the ^{7}Li(p,p'γ)^{7}Li reaction.
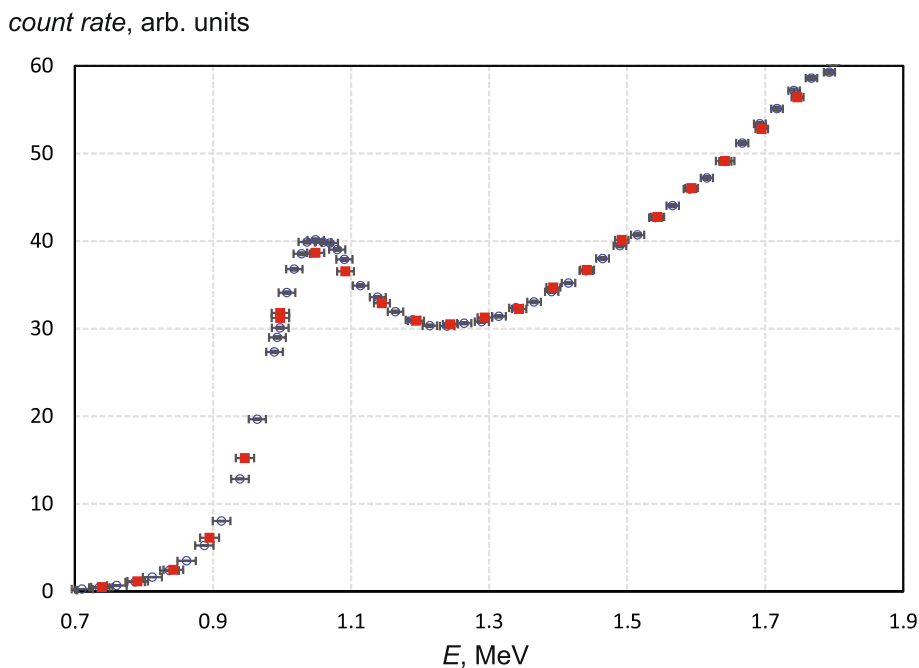
count rate, arb. units

Fig. 8. Measured dependence of the 478 keV photon count rate from a thin lithium target at proton energy *E*: ○ – emitted at the angle of 110°, □ – emitted at 15°.

1.85 MeV [21]. In the experiments performed, the lithium thickness was 200 μm.

Proton energy stability during the experiment was between 0.1 and 0.2%, average 0.14%. The absolute value of energy was calibrated according to the threshold of generation of neutrons of the ^{7}Li(p,n)^{7}Be reaction equal to 1.882 MeV. The 478 keV photons were measured for 2 min at each point, so that the error in measuring the count rate does not exceed 0.5%. Approximately the same measurement error was produced at measuring the charge carried by the proton beam, while the current stability of the proton beam was 3%. As a result, the measurement error

of the relative value of the photon yield shown in Fig. 5 did not exceed 1%. Measurement of the absolute photon yield is performed using a closed type Cs-137 radionuclide source of photon radiation, whose intensity reliability is 10%, and reference sources of photon radiation from the OSGI-TR set, whose intensity reliability is 7%. So, the absolute accuracy of measurement of γ -ray yield from a thick lithium target is determined by the reliability of Cs-137 source (10%), reference sources (7%), relative measurement accuracy (1%), and is about 15%.

Of all the previously measured or calculated data [4–8], the result obtained agrees only with the most recent result of measuring the
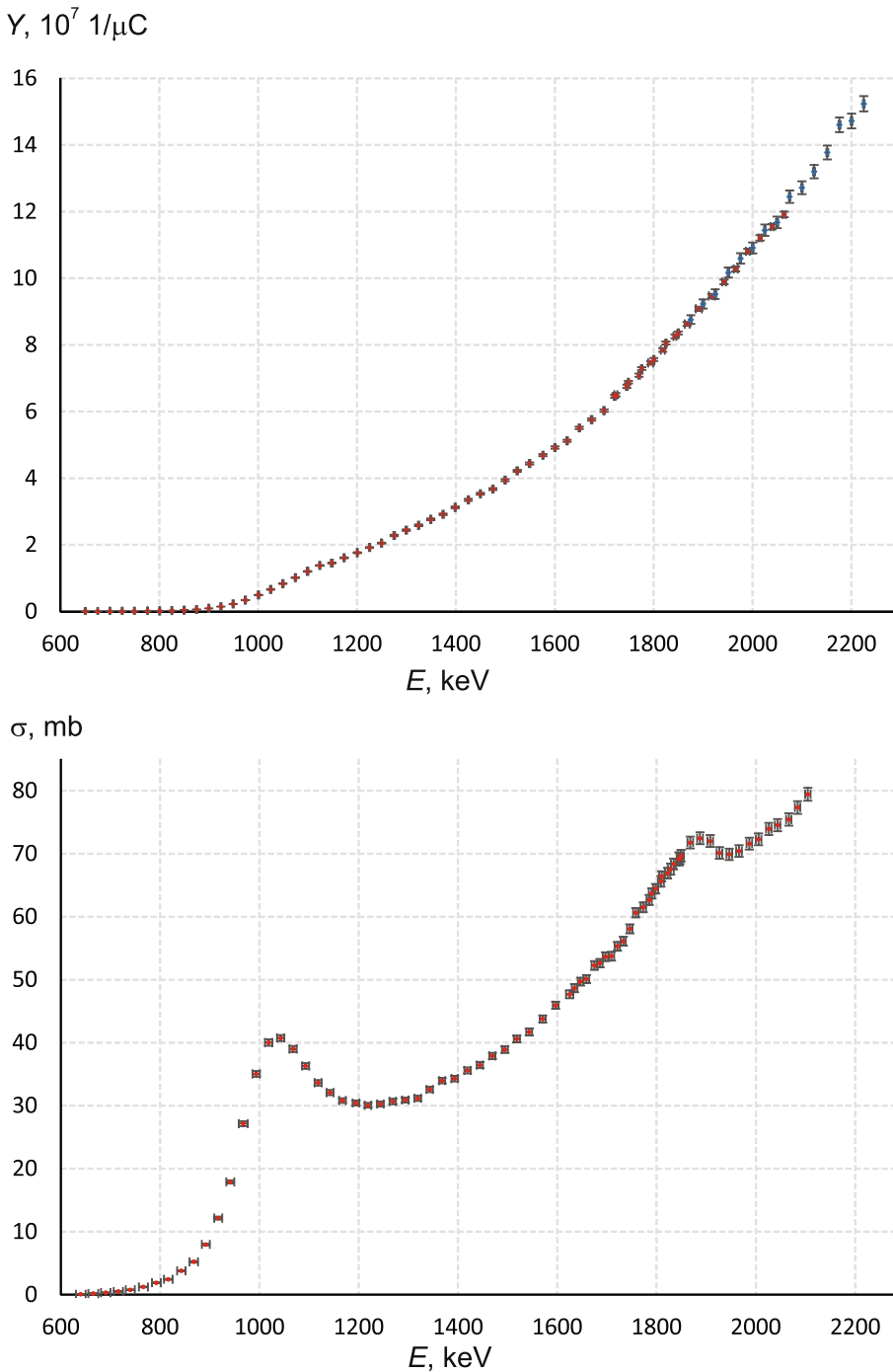
Y, 10^7 1/μC

σ, mb

photon yield at a proton energy of 1.67 MeV [8].

Then, in order to measure the cross-section of the ^{7}Li(p,p'γ)^{7}Li reaction a thin layer of lithium was evaporated on the copper disk and the yield of 478 keV photons was measured at proton energies from 0.7 to 1.85 MeV with the same 25 keV energy step in the same experimental geometry.

The thickness of the lithium layer is defined as follows. It is known that the rate of proton energy loss S in lithium depends on its energy E as [21]:

$$S = \frac{S_{low} \cdot S_{high}}{S_{low} + S_{high}} \text{ eV}/(10^{15} \text{ atoms/cm}^2), \text{ where } S_{low} = 1.6E^{0.45}, \text{ } S_{high} = \frac{725.6}{E}\ln(1 + \frac{3013}{E} + 0,04578E), E \text{ is taken in keV. Using this formula, let us}$$

calculate the amount of proton energy loss in lithium with crystal density. We obtain that passing through a one-micrometer layer the proton

loses 15.4 keV at 0.7 keV and 7.77 keV at 1.85 MeV. The photon yield from a thin lithium target is $Y_x = n \times \sigma I / e$, where $\times$ is the thickness of lithium, n is the density of lithium atomic nuclei (4.59·10^{22} cm^{-3}), σ is the ^{7}Li(p,p'γ)^{7}Li reaction cross-section, I is the proton beam current, e is the elementary charge. Since the 478 keV line count rates on a thin and thick targets were measured in 25 keV step in the same experimental geometry, the count rate Y_j of γ -quanta from a thick target can be determined from the measured count rate Y_i from a thin target as $Y_j = \sum_{i=0}^{j} Y_i \frac{25}{S_i(x)}$, where the index i indicates the measurement number ($i = 0$ at 0.7 MeV, $i = 1$ at 0.725 MeV and so on in 25 keV increments) and $S_i(x)$ is the value of the proton energy loss (in keV) in a lithium layer with thickness x. In the formula, the photon yield at a proton energy of 0.7 MeV is taken as a starting point, since the yield from the threshold at

Table 1
478 keV photon yield from a thick natural lithium target.

E, keV	ΔE, keV	Y, 10^7 μC^{-1}	ΔY, 10^7 μC^{-1}
650.2	1.2	0.00058	0.00008
675.5	0.9	0.0010	0.0001
700.1	1.0	0.0020	0.0002
724.9	0.9	0.0037	0.0002
749.5	1.0	0.0059	0.0002
776.2	1.1	0.0102	0.0002
800.6	1.1	0.0158	0.0003
825.5	1.1	0.0255	0.0003
850.2	1.2	0.0386	0.0005
875.4	1.2	0.0593	0.0006
900.1	1.1	0.0919	0.0007
924.6	1.2	0.143	0.0009
949.3	1.4	0.224	0.001
974.0	1.1	0.340	0.001
1000.6	1.4	0.496	0.002
1025.3	1.4	0.661	0.011
1050.0	1.6	0.834	0.008
1075.3	1.4	1.01	0.01
1099.9	1.8	1.20	0.01
1124.5	1.4	1.38	0.01
1149.0	2.0	1.45	0.01
1174.0	1.4	1.61	0.01
1200.6	1.2	1.76	0.01
1225.3	1.3	1.92	0.01
1249.7	1.2	2.05	0.01
1275.2	1.6	2.28	0.02
1299.7	1.6	2.44	0.02
1324.5	1.4	2.59	0.02
1349.2	1.4	2.77	0.02
1374.0	1.6	2.92	0.03
1398.5	1.3	3.12	0.03
1425.2	1.4	3.35	0.03
1449.6	1.5	3.53	0.03
1474.9	1.5	3.67	0.03
1499.6	1.5	3.94	0.03
1524.1	1.7	4.22	0.03
1549.1	1.6	4.44	0.03
1575.9	1.4	4.69	0.03
1600.5	1.5	4.92	0.03
1625.1	1.5	5.12	0.03
1649.6	1.5	5.51	0.03
1674.7	1.7	5.76	0.04
1699.7	1.5	6.03	0.04
1721.2	2.0	6.46	0.05
1723.7	3.1	6.50	0.05
1745.8	2.0	6.75	0.05
1749.1	1.5	6.88	0.04
1770.4	2.0	7.09	0.05
1775.8	1.4	7.29	0.04
1794.0	4.8	7.46	0.05
1800.3	1.4	7.56	0.04
1818.6	4.1	7.85	0.05
1824.9	1.6	8.05	0.04
1843.1	3.2	8.25	0.06
1849.7	1.7	8.36	0.04
1867.7	4.9	8.62	0.06
1875.2	1.7	8.76	0.13
1891.3	5.5	9.09	0.06
1900.1	2.0	9.23	0.14
1917.8	6.0	9.47	0.07
1924.6	1.7	9.52	0.14
1942.4	4.0	9.89	0.07
1951.2	1.7	10.17	0.15
1966.0	4.1	10.28	0.07
1975.8	1.5	10.60	0.16
1990.6	4.0	10.81	0.08
2000.4	1.8	10.91	0.16
2015.2	3.2	11.21	0.08
2024.9	1.5	11.44	0.17
2039.7	3.0	11.55	0.08
2049.8	2.3	11.68	0.18
2064.3	3.3	11.91	0.08
2075.1	1.6	12.45	0.19
2100.0	1.7	12.72	0.19

Table 1 (*continued*)

E, keV	ΔE, keV	Y, 10^7 μC^{-1}	ΔY, 10^7 μC^{-1}
2124.6	1.9	13.20	0.20
2151.3	1.8	13.78	0.21
2175.9	1.9	14.61	0.22
2200.4	1.8	14.72	0.22
2225.1	1.8	15.24	0.23

0.478 up to 0.7 MeV can be neglected. Fig. 6 presents two curves of the count rate from a thick target, one measured, and another reconstructed by the above formula with a thickness of lithium of 2.1 μm. In this case, the measured and reconstructed curves match the best, which means that lithium thickness is 2.10 ± 0.03 ± 0.30 μm, where the first error is the fitting error, the second is the systematic error due to the reliability of radionuclide sources of photon radiation.

Since the lithium thickness has been determined, measuring the 478 keV photon count rate allows us to determine the ^{7}Li(p,p'γ)^{7}Li reaction cross-section assuming that the radiation is isotropic; it is shown in Fig. 7. The relative error of the cross-section measurements is determined by the detector count rate error and charge stability, and it does not exceed 1%. The absolute cross-section error is determined by the reliability of radionuclide sources of photon radiation (as discussed above, and it does not exceed 15%) and the fitting error in measuring the thickness of lithium (1.5%). Although energy stability was better than 0.2%, slowing down of protons in the lithium layer of non-zero thickness increased the error in energy determination, which eventually ranged from 0.4 to 1.2%; it is shown in Fig. 7.

Pay attention to the fact that the cross section shown in Fig. 7 was obtained by multiplying the measured cross section by a factor of 1/0.925, taking into account the percentage of lithium-7 in natural lithium. Without multiplying by this factor, the measured cross section exactly coincides with the most recent results of Mateus [14], with the exception of four values at proton energies above 1.75 MeV.

4. Position B

Then measurements were taken at position B. The sensitive part of the spectrometer is located at a distance of 2.00 m at an angle of 15°.

The purpose of the measurement was to check the isotropy of the photon emission. In a previous work [13] it was argued that, if at 1030 keV resonance peak the radiation is isotropic, then at higher energy it will not. The largest dip in radiation intensity is predicted for an angle of 15°. So, at an energy of 1.8 MeV, as given in [13], the gamma-ray yield for thin target at this angle in the laboratory coordinate system is 3.5 times less than the yield at an angle of 120°. For a thick target this output ratio is given as 1.47. To check the isotropy of the radiation, the measurements were repeated at an angle of 15°. Fig. 8 shows the measured dependence of the radiation intensity at an angle of 15° and 110° from a thin target. It can be seen that no difference from isotropy is observed. The same result was obtained when measuring the intensity of radiation from a thick target: an increase in the proton energy from 1.4 to 1.8 MeV increases the radiation intensity by 2.45 ± 0.03 times both at an angle of 110° and 15°, while article [13] predicted an increase in radiation intensity by 1.94 times at an angle of 15°, 3.4 times at an angle of 90°, and 3.6 times at an angle of 120°.

5. Position C

For the measurements in position C the HPGe γ -ray spectrometer was located at a distance of 4.83 m and at an angle of 15° while the energy was below 1.882 MeV. For higher energies it was moved backward by 1.6 m and its sensitive volume was covered with cadmium. The NaI scintillator spectrometer was used in the whole energy range at a constant distance of 4.83 m. Placing the spectrometer in a separate room behind a thick wall made it possible to significantly reduce the

Table 2

^{7}Li(p,p'γ)^{7}Li reaction cross section.

E, keV	ΔE, keV	σ, mb	Δσ, mb
640.1	9.7	0.065	0.013
665.3	10.0	0.176	0.026
690.5	9.5	0.36	0.04
715.8	9.3	0.50	0.04
740.0	9.1	0.78	0.04
766.2	9.0	1.23	0.05
792.4	8.8	1.91	0.06
816.5	8.5	2.45	0.07
842.7	8.4	3.78	0.09
867.9	8.4	5.22	0.11
892.0	8.1	7.97	0.14
917.2	8.1	12.16	0.23
941.3	8.0	17.91	0.27
967.4	9.1	27.15	0.38
993.6	7.5	35.05	0.49
1018.7	7.4	40.03	0.50
1042.8	7.3	40.75	0.48
1067.9	7.1	39.01	0.47
1093.0	7.0	36.32	0.44
1118.2	6.9	33.64	0.43
1142.3	6.8	32.08	0.40
1167.4	6.7	30.82	0.39
1194.5	6.6	30.42	0.39
1218.6	6.5	30.07	0.39
1243.6	6.4	30.27	0.38
1268.7	6.4	30.68	0.42
1293.8	6.5	30.91	0.40
1318.9	6.4	31.17	0.40
1342.9	6.3	32.58	0.42
1368.1	6.0	33.97	0.43
1393.1	6.2	34.29	0.45
1419.2	6.1	35.59	0.48
1444.2	6.0	36.45	0.48
1469.3	6.0	37.90	0.50
1494.4	5.9	38.91	0.51
1518.5	5.9	40.60	0.53
1543.5	5.8	41.71	0.55
1570.6	5.7	43.77	0.56
1596.7	5.7	45.95	0.57
1624.7	7.3	47.67	0.63
1634.8	5.6	48.65	0.65
1646.8	5.6	49.70	0.64
1658.8	5.5	50.11	0.65
1674.9	6.0	52.27	0.70
1685.9	5.5	52.63	0.68
1696.9	5.5	53.65	0.70
1708.9	5.4	53.73	0.69
1721.0	5.4	55.31	0.70
1733.0	5.1	56.11	0.71
1746.0	5.4	58.08	0.72
1758.0	5.3	60.64	0.74
1773.1	5.3	61.48	0.78
1785.1	5.0	62.67	0.80
1790.0	5.9	63.70	0.83
1798.1	5.3	64.44	0.78
1808.7	5.9	65.61	0.85
1810.1	5.2	66.41	0.80
1822.2	5.2	66.91	0.84
1828.4	5.8	67.57	0.88
1834.2	4.9	68.37	0.86
1845.2	4.8	69.19	1.0
1847.2	5.2	69.21	0.83
1849.0	5.8	69.68	0.9
1867.7	5.7	71.77	0.9
1887.4	5.7	72.45	0.9
1908.0	5.7	72.01	0.9
1926.7	5.6	70.12	0.9
1946.3	5.6	69.91	0.9
1966.0	5.6	70.43	0.9
1986.6	5.5	71.60	0.9
2005.3	5.5	72.29	0.9
2026.0	5.5	73.94	1.0
2043.7	5.4	74.55	1.0
2066.3	5.4	75.44	1.0
2084.0	5.4	77.35	1.0
2104.6	5.3	79.44	1.0

background signal and to reduce the dead time of the HPGe spectrometer to a value not exceeding 4%.

Spectrometers were calibrated on total sensitivity by Be-7 source of 478 keV photons produced in the ^{7}Li(p,n)^{7}Be reaction. As a result of irradiation of a natural lithium target with a proton beam with an energy of 2100 ± 2 keV and a fluence of 3.602 ± 0.003C, 7.1 10^{14} ^{7}Be nuclei were produced [22]. Such a quantity of ^{7}Be nuclei decaying with a half-life of $t_{1/2}$ = 53.22 days, provides a source activity equal to $A = ln2\,N_{Be-7}/t_{1/2} = 0.693 \cdot 7.1 \cdot 10^{14}/(53.22 \cdot 86400) = 1.07 \cdot 10^8$ Bq. Since the branching ratio for the 478 keV emission in the decay is 10.3% the photon emission over 4π will be (1.10 ± 0.01) 10^7 s^{-1}. This calibration method is attractive due to the fact that the energy of the photons of the source is exactly equal to the energy of the registered photons and they are emitted from exactly the same place. Note that with such a calibration of the detector, the photon output at a proton energy of 1 MeV is 1.5% higher than the value obtained during calibration with a set of radionuclide sources (position A).

To measure the yield of photons from a thick lithium target, lithium 200 μm of thick was deposited, and to measure the reaction cross section, a lithium layer 1.23 ± 0.04 μm thick was deposited. The thickness of the thin lithium layer was determined in the same way as described above. Also, the thickness of the thin lithium layer was estimated by comparing the intensity of neutron radiation measured by a dosimeter BDMN-100–07 (Doza, Russia) from a thick and thin lithium target with proton energies from 1.95 MeV to 2.1 MeV. While the radiation intensity from a thick target increases with increasing proton energy [22], then from a thin target remains practically constant, repeating the cross section which changes slightly in this energy range: from 280 mb at 1.95 MeV to 316 mb at 2.1 MeV [23]. The lithium thickness estimated in this way is 1.16 ± 0.1 μm, which is in good agreement with the previous measurement.

The experimental results of the 478 keV photon yield from a thick natural lithium target and ^{7}Li(p,p'γ)^{7}Li reaction cross section obtained in C position are presented in Fig. 9, Table 1, and Table 2.

Comparing these results with the results presented in the "Position A" chapter, we conclude that the photon yield data are completely consistent with each other, the reaction cross sections are consistent at proton energies below 1.75 MeV and slightly higher at proton energies above 1.75 MeV. Also, in these measurements, the range of variation of the proton energy is expanded: the lower limit – from 0.7 MeV to 0.65 MeV, the upper – from 1.85 MeV to 2.225 MeV.

Let us also pay attention to the behavior of the ^{7}Li(p,p'γ)^{7}Li reaction cross section in the region of the threshold of ^{7}Li(p,n)^{7}Be reaction. Fig. 10 presents our results in comparison with the ones previously published [5,9,14]. We have confirmed the dip in the cross section even at forward angles where it was never measured before. The difference observed in the dip depth between the various authors could depend perhaps on the way the background is generated in the experimental set-up, recorded by the spectrometer and subtracted to the peak areas. In an earlier work [15], attention was drawn to the fact that only above 1.92 MeV, the background sharply increases. In our measurements, the background signal, as shown in Fig. 11, practically did not change when the proton energy increases from an energy 15 keV below the neutron generation threshold, by an energy 222 keV above the neutron generation threshold. Note that a signal from 511 keV photons appeared due to the ^{1}H(n, γ)^{2}H reaction and neutron activation of the copper substrate, but this signal was clearly separated from the useful one.

6. Conclusions

In this paper, a ^{7}Li(p,p'γ)^{7}Li reaction cross section and 478 keV photon yield from a thick lithium target at proton energies from 0.65 MeV to 2.225 MeV were measured with high precision. Adding cross section to the worldwide database is important for the boron neutron capture therapy because it helps refining the band of error and helps reducing unnecessary patient exposure. The data obtained can help
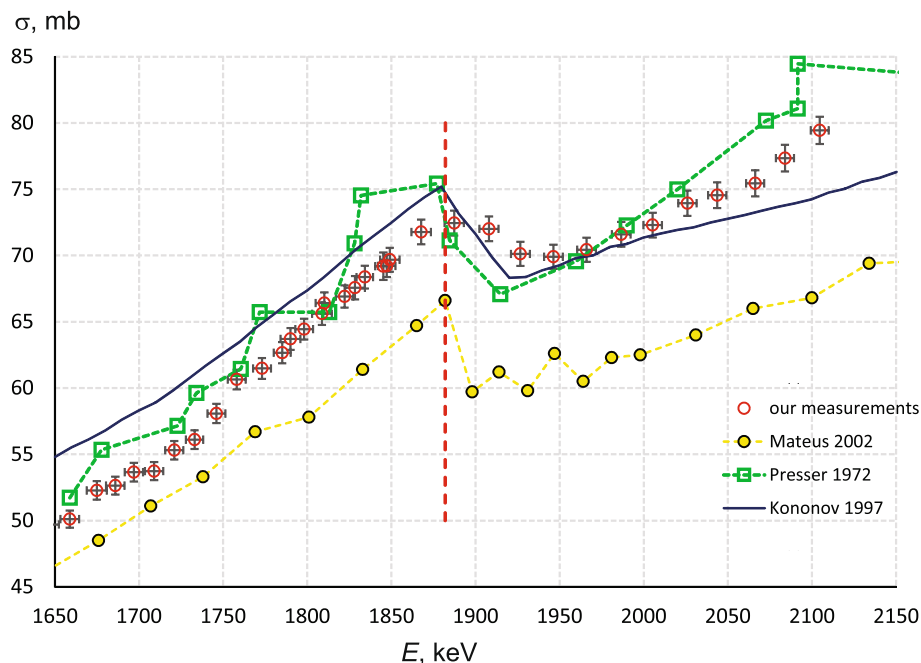
Fig. 10. Comparison of the results of measuring the $^7Li(p,p'\gamma)^7Li$ reaction cross section in the region of the threshold of $^7Li(p,n)^7Be$ reaction (indicated by the vertical line).
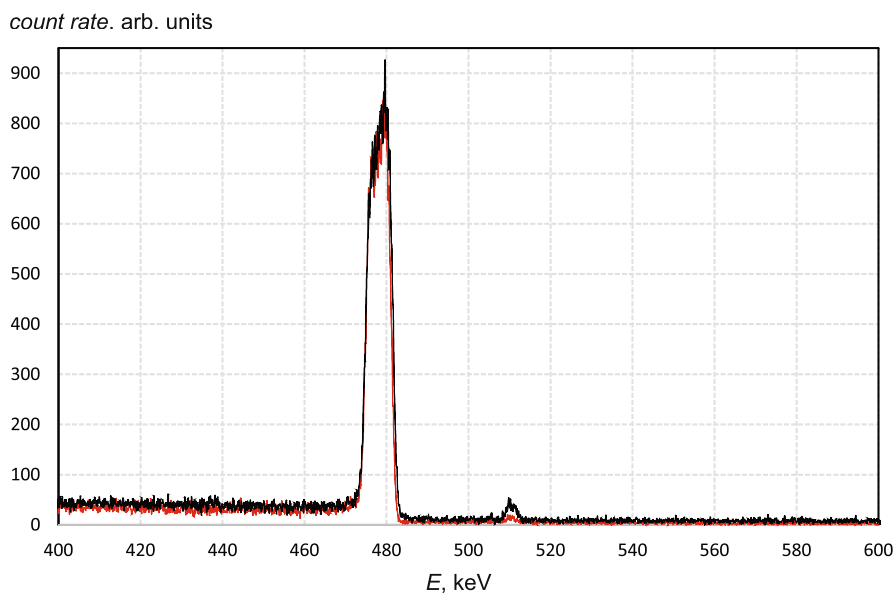

Fig. 11. Signal of HPGe γ-ray spectrometer at proton energy of 1.867 MeV (bottom red line) and 2.104 MeV (top black line). (For interpretation of the references to colour in this figure legend, the reader is referred to the web version of this article.)

establish a benchmark for radiation protection and treatment planning.

Funding

Data availability

The theoretical and experimental data presented in this work are available from the corresponding authors on reasonable request.

CRediT authorship contribution statement

Sergey Taskaev: Conceptualization, Supervision, Writing - review & editing. **Timofey Bykov:** Software. **Dmitrii Kasatov:** Investigation, Writing - original draft. **Iaroslav Kolesnikov:** Investigation. **Alexey Koshkarev:** Data curation. **Alexandr Makarov:** Validation. **Sergey Savinov:** Validation. **Ivan Shchudlo:** Investigation. **Evgeniia Sokolova:** Formal analysis.

Declaration of Competing Interest

The authors declare that they have no known competing financial interests or personal relationships that could have appeared to influence

the work reported in this paper.

References

[1] W.A.G. Saurwein, A. Wittig, R. Moss, Y. Nakagawa (Eds.). Neutron Capture Therapy: Principles and Applications. Springer, 2012, doi: 10.1007/978-3-642-31334-9.

[2] IAEA-TECDOC-1223. Current Status of Neutron Capture Therapy. International Atomic Energy Agency, Vienna, 2001.

[3] L. Zaidi, M. Belgaid, S. Taskaev, R. Khelifi, Beam shaping assembly design of ^{7}Li(p, n)^{7}Be neutron source for boron neutron capture therapy of deep-seated tumor, Appl. Radiat. Isotopes 139 (2018) 316–324, https://doi.org/10.1016/j.apradiso.2018.05.029.

[4] A. Anttila, R. Hanninen, J. Raisanen, Proton-induced thick-target gamma-ray yield for the elemental analysis of the Z = 3–9, 11–21 elements, J. Radioan. Chemistry 62 (1981) 293–306, https://doi.org/10.1007/BF02517360.

[5] V. Kononov, M. Bokhovko, O. Kononov, N. Kononova, Gamma-radiation of 7Li(p,n) 7Be neutron source, Preprint IPPE-2643, Obninsk, Russia (1997) (in Russian).

[6] A. Savidou, X. Aslanoglou, T. Paradellis, M. Pilakouta, Proton induced thick target γ-ray yields of light nuclei at the energy region E_p=1.0–4.1 MeV, Nucl. Instr. Meth. Phys. Res. B 152 152 (1) (1999) 12–18, https://doi.org/10.1016/S0168-583X(98)00962-8.

[7] C.L. Lee, X.-L. Zhou, R.J. Kudchadker, F. Harmon, Y.D. Harker, A Monte Carlo dosimetry-based evaluation of the ^{7}Li(p, n)^{7}Be reaction near threshold for accelerator boron neutron capture therapy, Med. Phys. 27 (1) (2000) 192–202, https://doi.org/10.1118/1.598884.

[8] T. Saito, T. Katabuchi, B. Hales, M. Igashira, Measurement of thick-target gamma-ray production yields of the 7Li(p, p')7Li and 7Li(p, γ)8Be reactions in the near-threshold energy region for the 7Li(p, n)7Be reaction, J. Nucl. Sci. Technol. 54 (2) (2017) 253–259, https://doi.org/10.1080/00223131.2016.1255576.

[9] G. Presser, R. Bass, Reactions ^{7}Li + n, ^{7}Li + p and excited states of the A = 8 system, Nucl. Phys. A 182 (2) (1972) 321–341, https://doi.org/10.1016/0375-9474(72)90281-3.

[10] F. Mozer, W.A. Fowler, C.C. Lauritsen, Inelastic scattertng of protons by Li^7, Phys. Rev. 93 (1954) 829–830, https://doi.org/10.1103/PhysRev.93.829.

[11] A.B. Brown, C.W. Synder, W.A. Fowler, C.C. Lauritsen, Excited states of the mirror nuclei, Li^7 and Be^7, Phys. Rev. 82 (1951) 159–180, https://doi.org/10.1103/PhysRev.82.159.

[12] EXFOR experimental nuclear reaction database.

[13] Aslam, W.V. Prestwich, F.E. McNeill, Thin target ^{7}Li(p, p'γ)^{7}Li inelastic gamma-ray yield measurements, J. Radioan. Nucl. Chem. 254 (2002) 533–544, https://doi.org/10.1023/A:1021646222974.

[14] R. Mateus, A.P. Jesus, B. Braizinha, J. Cruz, J.V. Pinto, J.P. Ribeiro, Proton-induced γ-ray analysis of lithium in thick samples, Nucl. Instr. Meth. Phys. Res. B 190 (2002) 117–121, https://doi.org/10.1016/S0168-583X(01)01222-8.

[15] H.W. Newson, R.M. Williamson, K.W. Jones, J.H. Gibbons, H. Marshak, Li^7(p, n), (p, p'γ), and (p,γ) reactions near neutron threshold, Phys. Rev. 108 (1957) 1294–1300, https://doi.org/10.1103/PhysRev.108.1294.

[16] D. Bachiller Perea, P. Corvisiero, D. Jiménez Rey, V. Joco, A. Maira Vidal, A. Muñoz Martin, A. Zucchiatti, Measurement of gamma-ray production cross sections in Li and F induced by protons from 810 to 3700 keV, Nucl. Instr. Meth. Phys. Res. B 406 (2017) 161-166, doi: 10.1016/j.nimb.2017.02.017.

[17] S.Y. Taskaev, Development of an accelerator-based epithermal neutron source for boron neutron capture therapy, Phys. Part. Nucl. 50 (5) (2019) 569–575, https://doi.org/10.1134/S1063779619050228.

[18] B. Bayanov, V. Belov, V. Kindyuk, E. Oparin, S. Taskaev, Lithium neutron producing target for BINP accelerator-based neutron source, Appl. Radiat. Isotopes 61 (5) (2004) 817–821, https://doi.org/10.1016/j.apradiso.2004.05.032.

[19] Handbook of Stable Isotope Analytical Techniques. Volume II (2009) 1123-1321, doi: 10.1016/B978-0-444-51115-7.00028-0.

[20] K. Lieberman, G.J. Alexander, J.A. Sechzer, Stable isotopes of lithium: dissimilar biochemical and behavioral effects, Experientia 42 (9) (1986) 985–987, https://doi.org/10.1007/BF01940701.

[21] H. Andersen, J. Ziegler. Hydrogen stopping powers and ranges in all elements. Volume 3 of the stopping and ranges of ions in matter. New York, Toronto, Oxford, Sydney, Frankfurt, Paris: Pergamon Press Inc., 1997.

[22] C.L. Lee, X.-L. Zhou, Thick target neutron yields for the ^{7}Li(p, n)^{7}Be reaction near threshold, Nucl. Instr. Meth. Phys. Res. B 152 (1) (1999) 1–11, https://doi.org/10.1016/S0168-583X(99)00026-9.

[23] Nuclear Reaction Data Library ENDF/B-VIII.0.